
MoleHD: Automated Drug Discovery using Brain-Inspired Hyperdimensional Computing

Dongning Ma

Department of Electrical and Computer Engineering
Villanova University
Villanova, PA 19085
dma2@villanova.edu

Xun Jiao

Department of Electrical and Computer Engineering
Villanova University
Villanova, PA 19085
xun.jiao@villanova.edu

Abstract

Modern drug discovery is often time-consuming, complex and cost-ineffective due to the large volume of molecular data and complicated molecular properties. Recently, machine learning algorithms have shown promising results in virtual screening of automated drug discovery by predicting molecular properties. While emerging learning methods such as graph neural networks and recurrent neural networks exhibit high accuracy, they are also notoriously computation-intensive and memory-intensive with operations such as feature embeddings or deep convolutions. In this paper, we propose a viable alternative to neural network classifiers. We present MoLeHD, a method based on brain-inspired hyperdimensional computing (HDC) for molecular property prediction. We first transform the SMILES presentation of molecules into feature vectors by SMILE-PE tokenizers pretrained on the ChEMBL database. Then, we develop HDC encoders to project such features into high-dimensional vectors that are used for training and inference. We perform an extensive evaluation using 30 classification tasks from 3 widely-used molecule datasets and compare MoLeHD with 10 baseline methods including 6 SOTA neural network classifiers. Results show that MoLeHD is able to outperform all the baseline methods on average across 30 classification tasks with significantly reduced computing cost. To the best of our knowledge, we develop the first HDC-based method for drug discovery. The promising results presented in this paper can potentially lead to a novel path in drug discovery research.

1 Introduction

Drug discovery is the process of using multi-disciplinary knowledge such as biology, chemistry and pharmacology to discover proficient medications amongst candidates according to safety and efficacy requirements. Modern drug discovery often features a virtual screening process to select candidates from general chemical databases such as *ChEMBL* [6] and *OpenChem* [16] to build a significant smaller in-house database for further synthesis. Traditional virtual screening based on computational methods such as similarity searching [3] and pharmacophere mapping [35] are facing stronger obstacles due to the growing magnitude of data. Therefore, data-driven machine

learning techniques are increasingly applied into drug discovery, particularly in predicting molecular properties with drug discovery objectives from very large volume of data.

Traditional machine learning algorithms such as random forest [12], support vector machine [21] and k nearest neighbors [1] and gradient boosting [40], are introduced in drug discovery applications first. Such algorithms use molecular representations as input to predict molecular properties. However, because of limited sophistication, deep and complex structural information within a molecule is generally overlooked by those models. Thus, they typically do not exhibit strong capability in learning the features and can only achieve sub-par performance in predicting molecule properties.

On the other hand, inspired by the recent success from other applications such as computer vision, neural network models have been increasingly applied in drug discovery. As the 2-D structures of molecules are essentially graph-like patterns with atoms (nodes) and bonds (edges), graph neural networks (GNNs) can be naturally applied. GNN learns representations by aggregating nodes and neighbouring information for molecular property predictions under different drug discovery objectives. However, molecular graphs often requires pre-processing or featurization. Extended-connectivity fingerprints (ECFP) is one of the most common featurization method that converts molecular graphs into fixed length representations, or fingerprints [33]. Such featurization algorithms usually requires comprehensive efforts using chemical tool-chains such as RDKit [19].

With such motivation, this paper takes a radical departure from traditional machine learning methods including neural networks by developing a brain-inspired hyperdimensional computing (HDC) model that requires less pre-processing efforts and is easier to implement. Inspired by the attributes of brain circuits including high-dimensionality and fully distributed holographic representation, this emerging computing paradigm postulates the generation, manipulation, and comparison of symbols represented by high-dimensional vectors, e.g., 10,000 dimensions. Compared with DNNs, the advantages of HDC include smaller model size, less computation cost, and one/few-shot learning, making it a promising alternative, especially in low-cost computing platforms [14]. Recently, HDC has already demonstrated success on various application domains such as language classification [31], industrial systems [17], robotics [26], biosignal analysis [30], and biological sequence matching [10].

In this paper, we develop Mo1eHD, a new algorithm based on hyperdimensional computing to predict molecular properties during virtual screening in drug discovery. The qualitative advantages of Mo1eHD compared to existing neural network-based classifiers for drug discovery are: (1) backpropagation-free: Mo1eHD does not need backpropagation to train a set of parameters; instead, it uses one/few-shot learning to establish abstract patterns that can represent specific symbols (just like human brains). (2) efficient computing: unlike neural networks, Mo1eHD does not need complicated arithmetic operations such as convolutions which presents a major computing/energy burden to computing platforms; instead, it only uses simple arithmetic operations such as addition between two vectors. Thus, Mo1eHD only needs to run on commodity CPU and can finish both training and testing on the reported datasets within minutes, while GNN requires around 5 days for just training using Nvidia GPU [37]. (3) smaller memory footprint: Mo1eHD only needs to store a set of vectors for comparison during inference which is usually less than 10 MB, while SOTA neural networks often need millions of nodes and requires memory in 100MB scale to just store the parameters (e.g., weights and activation values) [23].

The main contributions of this paper are summarized as below:

1. We take a radical departure from traditional learning methods and neural networks to develop a drug discovery algorithm based on the emerging brain-inspired hyperdimensional computing. To the best of our knowledge, Mo1eHD is the first application of HDC in drug discovery. This promising results of Mo1eHD provide a viable option and alternative to neural networks in drug discovery domain.
2. We develop a complete pipeline for HDC-based drug discovery. First, Mo1eHD tokenizes SMILE strings into tokens representing the substructures and then project them into hypervectors during encoding. Then, Mo1eHD uses the encoded hypervectors to train the classification model. During inference, the test sample is encoded into HV and is compared with the pre-trained HVs for classification.
3. We performed an extensive evaluation using Mo1eHD on 30 classification tasks from 3 widely-used molecule datasets and compare it with 10 baseline methods (6 of which are SOTA neural network classifiers). Experimental results show that Mo1eHD is able to outperform

all the baseline methods including graph/recurrent neural networks on average across 30 classification tasks.

2 Related Works

Since HDC was proposed as a learning method by P. Kanerva [13], researches have been focusing on two lines. The first line is about application of HDC. HDC has been used in modern robotics to perform active perception by integrating the sensory perceptions experienced by an agent with its motoric capabilities, which is vital to autonomous learning agents [26]. HDC has also been used in bio-medical signal processing by exhibiting 97.8% accuracy on hand gesture recognition based on EMG, which surpasses support vector machine by 8.1% [30]. Another line of research has been focusing on improving the efficiency of HDC models on hardware. *QuantHD* [9] proposed quantized HDC models with improved accuracy over binarized HDC. *CompHD* compresses the HDC model size with minimal loss of accuracy [27]. Several works have also explored emerging architecture such as resistive memory for implementing HDC models [11, 39, 34]. Machine learning algorithms are used in drug discovery mostly in predicting molecular properties to determine if they satisfy the drug discovery objective. Earlier works focus on traditional ML algorithms such as logistic regression [40], random forest [12] and support vector machine [21]. However, because of model limitations, such traditional models generally achieve inferior performance. More recent works apply emerging machine learning algorithms such as graph neural networks(GNN) for achieving higher performance. GNNs leverages fingerprints derived from the molecular graph to learn the representations. Direct message passing neural network (D-MPNN) is an evolution of message passing neural networks that centers on bonds between atoms which is able to maintain two representations [41, 36]. Contrastive learning is also applied into GNN to fuse drug discovery domain knowledge and molecular properties to augment learning of representations [5, 37]. In addition to GNNs, natural language processing (NLP) models such as recurrent neural networks (RNN) are also introduced in drug discovery. Compared with GNNs, RNNs typically do not rely on complex fingerprint conversion process using toolchains such as **RDKit**, which accelerates the learning process [29, 22]. However, RNNs still require word embeddings tools such as **Smi2Vec**, to fully extract features from the a molecule SMILES representation.

3 Preliminaries on HDC

In this section, we introduce the preliminaries of HDC including basic concepts and notions, operations and similarity measurement.

3.1 Hypervectors

Hypervectors (HV) are high-dimensional (usually higher than 10,000), holographic (not micro-coded) vectors with (pseudo-)random and i.i.d. elements [13]. An HV with d dimensions can be denoted as $\vec{H} = \langle h_1, h_2, \dots, h_d \rangle$, where h_i refers to the elements inside the HV. HVs are fundamental blocks in HDC that are able to accommodate and represent information in different scales and layers. When the dimensionality is sufficiently high (e.g., $D = 10,000$), any two random HVs are nearly orthogonal [13]. HDC utilizes different operations HVs support as means of producing aggregations of information or creating representations of new information.

3.2 Operations

In HDC, addition (+), multiplication (*) and permutation (ρ) are the three basic operations HVs can support as illustrated in Eq. 1. Additions and multiplications take two input HVs as operands and perform **element-wise** add or multiply operations on the two HVs. Permutation takes one HV as the

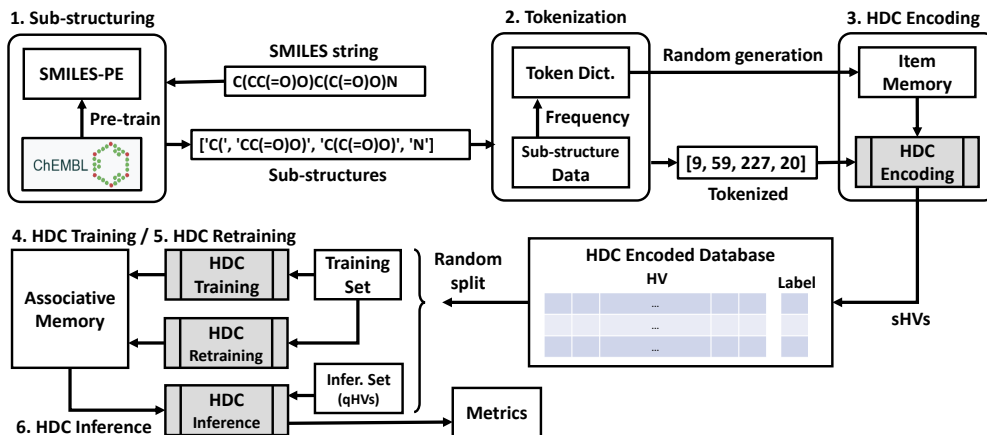


Figure 1: Overview of Mo1eHD. Mo1eHD has six major steps: **Sub-structuring** and **Tokenization** for pre-processing; **Encoding**, **Training**, **Retraining** and **Inference** for HDC processing.

input operand and perform **cyclic rotation**. All the operations do not modify the dimensionality of the input HVs, i.e. the input and the output HVs are in the same dimension.

$$\begin{aligned}
 \vec{H}_p + \vec{H}_q &= \langle h_{p1} + h_{q1}, h_{p2} + h_{q2}, \dots, h_{pd} + h_{qd} \rangle \\
 \vec{H}_p * \vec{H}_q &= \langle h_{p1} * h_{q1}, h_{p2} * h_{q2}, \dots, h_{pd} * h_{qd} \rangle \\
 \rho_1(\vec{H}) &= \langle h_d, h_1, h_2, \dots, h_{d-1} \rangle
 \end{aligned}
 \tag{1}$$

These three HD operations also have their corresponding physical meanings. Addition is used to aggregate same-type information, while multiplication is used to combine different types of information together to generate new information. Permutation is used to reflect spatial or temporal changes in the information, such as time series or spatial coordinates [13].

3.3 Similarity Measurement

In HDC, the similarity metric δ between the information that two HVs represent is measured by similarity check. Different algorithms can be used to calculate the similarity, such as the Euclidean (L_2) distance, the Hamming distance (for binary HVs), and cosine similarity (which we use in this paper as noted in Eq. 2). A higher similarity δ between two HVs shows that these two HVs have more information in common, or vice versa. Because of the high dimensionality of HVs, addition generally results in a new HV that is approximately 50% similar to the two original HVs, while multiplication and permutation result in HVs that are orthogonal to the original HVs, i.e., not similar.

$$\delta(\vec{H}_p, \vec{H}_q) = \frac{\vec{H}_p \cdot \vec{H}_q}{\|\vec{H}_p\| \times \|\vec{H}_q\|} = \frac{\sum_{i=1}^d h_{pi} \cdot h_{qi}}{\sqrt{\sum_{i=1}^d h_{pi}^2} \cdot \sqrt{\sum_{i=1}^d h_{qi}^2}}
 \tag{2}$$

4 Mo1eHD Framework

In this section, we will introduce the proposed framework Mo1eHD and how it utilizes HDC to perform learning tasks in drug discovery. An overview of Mo1eHD is presented in Fig. 1.

4.1 Sub-structuring

In Mo1eHD, sub-structuring is the process of dividing a SMILES string into its sub-structures for future tokenization. The primary input to Mo1eHD is the simplified molecular-input line-entry system (SMILES) format string of a compound or molecule. SMILES is a notation system for modern chemical information processing [38]. Its advantages including linear and ASCII-only notation as

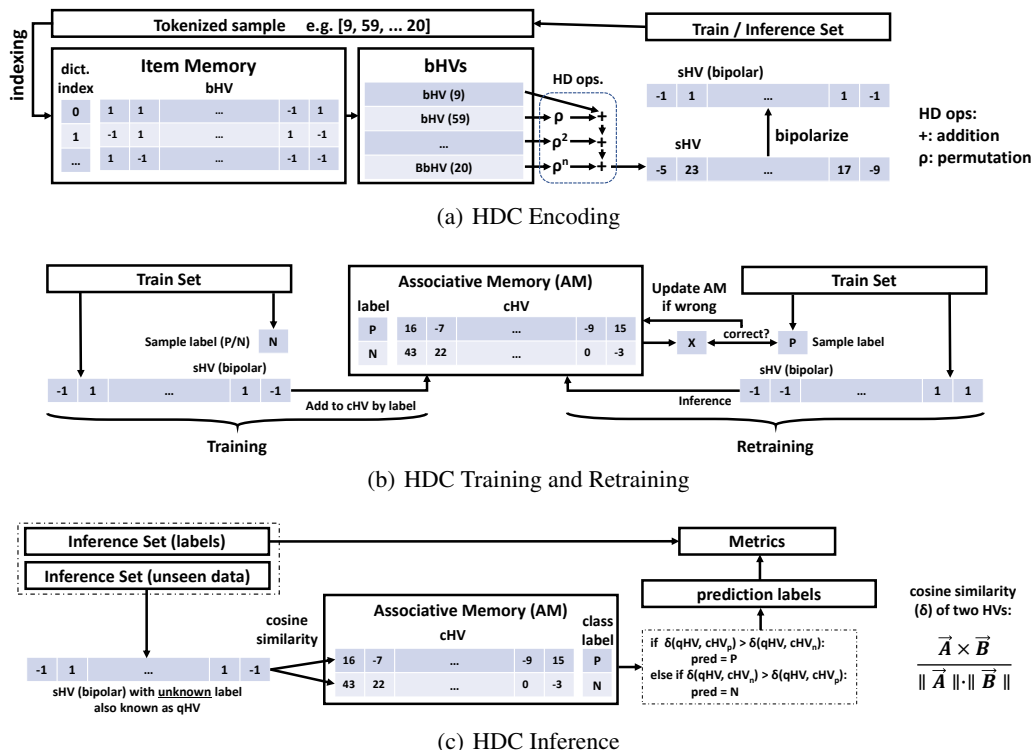


Figure 2: HDC processing: Encoding, training, retraining and inference.

well as easy conversion from/to the 2-D structure make it a primary method for molecule analysis particularly in drug discovery applications [28, 8, 4].

MoleHD then uses the SMILES Pair Encoding (SMILES-PE) model to mine the sub-structures in the input SMILES strings. SMILES-PE is a novel data-driven algorithm to find substructures from a SMILES string [20]. MoleHD uses the open-source SMILES-PE pre-trained from a large volume of chemical database such as ChEMBL for learning the frequently appeared sub-string patterns to tokenize a SMILES string into sub-structures, so it can be used as-is and does not require additional engineering effort.

4.2 Tokenization

Tokenization is the process of assigning unique identifier to the sub-structures according to their frequency ranking. MoleHD performs statistical analysis to rank the sub-structures from all the available data according to their occurrence frequency, and uses their rank to convert the sub-structures into a list of numbers. The substructures along with their rank are recorded to establish the token dictionary. However, only the top- m most frequent sub-structures will be stored due to token dictionary size limitations or other user-specific constraints. For missing sub-structures, a special token '0' is assigned.

4.3 HDC Encoding

Encoding is the process to project real-world features into their high-dimensional space representations: the HVs. In MoleHD, encoding process projects tokenized sample into its representing sample HV (sHV, or \vec{S}) via a combination of pre-defined HD operations as shown in Fig. 2(a).

Item Memory Item memory is generated from the token dictionary in tokenization. The item memory contains base HVs (bHV, or \vec{B}) in the same number ($m + 1$, considering the missing entry assigned as '0') as the entries in the token dictionary, i.e., each HV serves as the high-dimensional

representation of a token. The item memory is fully random generated using a seed to ensure the i.i.d. properties. We note item memory as $\mathbb{B} = \{\vec{B}_0, \vec{B}_1, \dots, \vec{B}_m\}$ where \vec{B}_i is the base HV with index i .

HD operations in Encoding In MoLeHD, encoding schemes can be flexible and data-specific. Here as an example, we are following a unigram-based encoding scheme described as Algorithm 1. Tokenized sample first uses its tokens iteratively in the item memory to index and fetch the corresponding base HVs. The base HVs permute by their order in the tokenized sample and added up to establish the sample HV (Line 2 - 4). MoLeHD also bipolarizes the elements inside the sample HV according to their relation with zero (Line 5 - 11).

When all the available data are encoded, we can build an encoded database for all the corresponding sample HVs along with their labels. We then perform random split over the database to obtain the training set and inference set of HVs. We use \vec{S}_l to represent a sample HV with label l

Algorithm 1 MoLeHD Encoding Algorithm

Input tokenized sample $T = \{t_0, t_1, t_k\}$, item memory \mathbb{B} .

Output sample HV \vec{S}

```

1: setZero( $\vec{S}$ )
2: for  $t_i$  in  $T$  do Perform uni-gram encoding. */
3:    $\vec{S} = \vec{S} + \rho^i(\vec{B}_{t_i})$ 
4: end for
5: for  $s_i$  in  $\vec{S}$  do Bipolarize the sample HV. */
6:   if  $s_i > 0$  then  $s_i = 1$ 
7:   else if  $s_i < 0$  then  $s_i = -1$ 
8:   end if
9: end for

```

4.4 HDC Training

Training is the process of establishing the associative memory $\mathbb{C} = \vec{C}_1, \vec{C}_2, \dots, \vec{C}_p$ using the training set. Associative memory (AM) contains p class HVs (cHV, or \vec{C}), each representing a class in a learning task. Using a binary classification task as example shown in Fig. 2(b), AM contains the class HV representing positive (P) and negative (N). For each training sample, MoLeHD adds its HV to the corresponding class HV according to the label, as shown in Eq. 4. This process is to aggregate the information from sample HVs together into the AM. However, one-epoch training is usually not enough to train a reliable AM for learning tasks, it is necessary to perform additional epochs for fine-tuning or retraining.

$$\vec{C}_P = \sum \vec{S}_p, \quad \vec{C}_N = \sum \vec{S}_n \quad (3)$$

4.5 HDC Retraining

Retraining is the process of fine-tuning the associative memory to enhance its accuracy using the training set, as shown in Fig. 2(b). For each training sample, MoLeHD tries to use the AM to predict its label. If the prediction is correct, MoLeHD proceeds to the next training sample. However, if the prediction is wrong, it indicates that the correct information of the sample HV has not been aggregated into the AM, or the information in the AM is properly represented. Therefore, MoLeHD performs an update to the AM to remove the erroneous and add the correct information. by subtracting the sample HV from the wrongly predicted class HV and add it to the correct class HV, as shown in Eq. 4.

$$\vec{C}_{wrong} = \vec{C}_{wrong} - \vec{S}, \quad \vec{C}_{correct} = \vec{C}_{correct} + \vec{S} \quad (4)$$

4.6 HDC Inference

Inference is the process of using unseen data from the inference set to evaluate the trained model's performance. As illustrated in Fig. 2(c), MoLeHD calculates the cosine similarity (δ) between the

sample HV from the inference set with unknown label (referred to as query HV (qHV), $\vec{Q}_?$) and each cHV in the AM to obtain the similarity values. The cHV with the most similarity indicates having the most overlap as to the preserved information with the qHV. Therefore, class of the qHV, i.e., the class of the inference sample, is subsequently predicted as x , summarized as Eq. 5.

$$x = \operatorname{argmax}(\delta(\vec{Q}_?, \mathbb{C})) \quad (5)$$

5 Experimental Results

5.1 Experimental Setup

Datasets We use 30 binary classification tasks in total from 3 datasets in the popular **MoleculeNet** benchmark (under MIT license) for molecule machine learning [40]. For each dataset, we perform 0.8/0.2 random split to build our training and inference set and repeat 10 experiments to get average performance with error bars presented in Table 1. Details of datasets are as follows:

- **BBBP** [24]: contains 2052 drug compounds and their binary label (positive or negative) of permeability to the blood-brain barrier.
- **Clintox** [7]: contains 1491 drug compounds and their binary label (positive or negative) of 1) clinical trial toxicity and 2) FDA approval status.
- **SIDER** [18]: contains 1428 marketed drugs and their adverse drug reactions (ADR) in 27 individual tasks per **MedDRA** classifications [2]. Each of the 27 tasks aims to classifying the positive (active) or negative (inactive) relationship between the drug compound and the ADR disorders of system organs. Table 2 lists the corresponding system organs of each task.

Baseline Algorithms We compare Mo1eHD with various baseline methods. They can be classified into two groups. The first group features basic machine learning algorithms like logistic regression (LR), random forest (RF) and support vector machine (SVM). Basic learning algorithms are generally easier to implement, smaller in model size, and usually do not require extensive pre-processing for the inputs, although their capability may be limited. The second group features more advanced SOTA algorithms, including different graph convolutional neural network models, recurrent neural network models and hybrid models. Those models have stronger capabilities in classification, but require sophisticated data pre-processing such as embedding or vectorization, large model size, and higher memory footprints.

- **Basic ML Algorithms** including **LR**, **RF** (with 10 classifiers), **SVM** and gradient boosting (**XGBoost**) implemented and reported in the *MoleculeNet* benchmark [40] and *DeepChem* [32] framework.
- **Weave**, which is a graph convolution method that takes both local chemical environment and atom connectivity in featurization [15].
- **MolCLR**, which is a graph neural network with contrastive learning of representations with augmentations of atom masking, bond deletion, and subgraph removal [37].
- **D-MPNN** [41, 36], which is the directed message passing neural network that operates on molecular graphs. It centers messages on bonds instead of atoms like general MPNNs, maintaining two representations for the message centered on the bond between atoms.
- **CK-GNN**, which is the contrastive knowledge-aware graph neural network for self-supervised molecular representation that learns to fuse domain knowledge into molecular graph representation, also with molecule cluster strategy introduced in the framework [5].
- **LSTM**, which applies a modified version of the Smi2Vec tool to convert SMILE strings into atom vectors and then apply long short term memory (LSTM) recurrent neural networks for classification tasks [29].
- **BiGRU**, which also uses Smi2Vec. It leverages the bidirectional gated recurrent unit (BiGRU) recurrent neural network to train sample vectors embedded in the atomic matrix [22].

5.2 Metrics

Drug discovery datasets are mostly significantly imbalanced, thus accuracy is generally not considered as a valid metric to reflect performance of a model. Receiver operating characteristics (ROC) curves and ROC Area-under-curve (AUC) scores are mostly embraced as the metric for model prediction performance, as suggested by benchmark datasets along with majority of literature [40, 32, 25]. Since HDC models are predicting using similarities, the “probability” used in calculating the ROC-AUC score requires specific definition. We propose to use “confidence level” (for being positive) η in Eq. 6s. Confidence level is derived from similarities between query HV and the class HVs. The larger the difference, the higher the confidence of the HDC model prediction. Because the range of similarity difference is [-2, 2], to perform linear transformation to map the range of confidence level to [0, 1], we accordingly set 1/2 as the average value and 1/4 for coefficient of similarity difference, conforming with the probabilities.

$$\eta = \frac{1}{2} + \frac{1}{4}(\delta(\vec{Q}_?, \vec{C}_P) - \delta(\vec{Q}_?, \vec{C}_N)) \quad (6)$$

5.3 MoLeHD vs. Baseline Models

As shown in Table 1, we present the comparison between MoLeHD and the baseline machine learning models, which shows that MoLeHD is able to achieve the highest average ROC-AUC score (0.837) among all baseline methods, outperforming the second place (D-MPNN[36]) by more than 2%. For fair comparison, MoLeHD and baselines are compared out-of-box, i.e., using the default parameters presented in the literature. For some models, we also mentioned their elaborations such as the neural network structures and the number of nodes in each layer.

Table 1: Model performance (ROC-AUC score on inference set) on **BBBP**, **Clintox**, and **SIDER** datasets, and elaborations. “-” means either the data is not available in the paper or not applicable.

Model	BBBP	Clintox	SIDER	Average	Model Elaboration
LR[40]	0.699±0.002	0.722±0.039	0.643±0.012	0.688	-
RF[40]	0.803±0.036	0.551±0.039	0.567±0.008	0.640	#classifiers: 10
SVM[40]	0.729±0.000	0.669±0.092	0.507±0.012	0.635	-
XGBoost[40]	0.696±0.000	0.799±0.050	0.656±0.027	0.717	-
Weave[40]	0.671±0.014	0.832±0.037	0.581±0.027	0.695	Weave:6*(50),FC:(2000,100)
MolCLR[37]	0.736±0.005	0.932±0.017	0.68±0.011	0.783	GIN: 5*(512,), MLP: (256,)
D-MPNN[36]	0.919±0.027	0.897±0.029	0.632±0.027	0.816	GNN: 3*(300,)
CK-GNN[5]	0.907	0.781	0.660	0.783	GNN: (512,256)
LSTM[29]	0.832	-	0.530	0.681	-
BiGRU[22]	0.854	0.978	0.607	0.813	GRU: (200,)
MoleHD	0.892±0.013	0.965±0.008	0.654±0.011	0.837	HV dim: 10,000

MoLeHD vs. Traditional Models From Table 1, we can observe that MoLeHD is able to outperform almost all the traditional machine models across all the datasets, with only marginal loss against **XGBoost** in **SIDER**. The average ROC-AUC score of MoLeHD is also more than 0.12 to 0.27 higher than the traditional models, which is a huge improvement from the baseline models from the **MoleculeNet** benchmark.

MoLeHD vs. NN Models In addition to dominating over the traditional models, MoLeHD also shows advantages compared with the SOTA neural network models. Although MoLeHD is not the best performer in each application individually, the application-average score of MoLeHD is the highest. In addition, while some neural network models are able to achieve high accuracy on specific dataset such as **BiGRU** on **Clintox** and **D-MPNN** on **BBBP**, they have significantly inferior score on other dataset evaluated. This indicates such models can be particularly specialized in one or few applications. MoLeHD, on the contrary, shows more stable score across different applications and constantly ranks close to top amongst all the datasets.

Task-by-task Comparison For **SIDER** dataset, we present a more detailed, task-by-task comparison amongst four models: two traditional machine learning models **RF** and **SVM** [40], and

two SOTA neural network models **LSTM** and **BiGRU** [29, 22] which have the task-specific data available. Mo1eHD is able to achieve higher score than **RF**, **SVM** and **LSTM** in 26 tasks out of 27 tasks. Compared with the more recent model **BiGRU**, Mo1eHD is still able to achieve higher score in 21 tasks. On average, Mo1eHD achieves 0.046 – 0.146 higher ROC-AUC score than other four models compared here.

Table 2: Model performance (ROC-AUC score on inference set) on 27 tasks of the **SIDER** dataset.

Task	RF	SVM	LSTM	BiGRU	MoleHD
Hepatobiliary	0.5654	0.5553	0.5843	0.6504	0.6952
Metabolism and nutrition	0.5490	0.5083	0.5345	0.5998	0.6668
Product issues	0.4906	0.5032	0.5048	0.5662	0.7589
Eye	0.5034	0.5071	0.5087	0.6044	0.6334
Investigations	0.4877	0.5014	0.5045	0.6674	0.5821
Musculoskeletal and connective tissue	0.5180	0.5116	0.5620	0.5533	0.6247
Gastrointestinal	0.5551	0.4926	0.5564	0.6629	0.7303
Social circumstances	0.4828	0.4918	0.5170	0.6089	0.7001
Immune system	0.5558	0.5024	0.5248	0.5770	0.5132
Reproductive system and breast	0.5436	0.5601	0.5956	0.6061	0.7125
Neoplasms	0.5363	0.5388	0.5396	0.5818	0.6153
General and administration site conditions	0.4922	0.4826	0.4929	0.5884	0.7287
Endocrine	0.5245	0.4920	0.5323	0.5873	0.6811
Surgical and medical procedures	0.5228	0.4955	0.4960	0.5642	0.5529
Vascular	0.4976	0.5036	0.5011	0.5303	0.7183
Blood and lymphatic system	0.5373	0.5036	0.5408	0.6000	0.6130
Skin and subcutaneous tissue	0.5417	0.4959	0.5642	0.6683	0.7927
Congenital, familial and genetic	0.4713	0.4971	0.5000	0.6084	0.5878
Infections and infestations	0.5139	0.4989	0.5148	0.6621	0.6528
Respiratory, thoracic and mediastinal	0.4893	0.5122	0.4954	0.6250	0.6485
Psychiatric	0.5282	0.5073	0.5378	0.5861	0.6477
Renal and urinary	0.5632	0.5137	0.5767	0.6173	0.6291
Pregnancy, puerperium and perinatal conditions	0.4769	0.4962	0.4961	0.5164	0.6370
Ear and labyrinth	0.5617	0.5000	0.5012	0.6395	0.6778
Cardiac	0.5530	0.4899	0.5734	0.5918	0.6554
Nervous system	0.4890	0.5417	0.5147	0.7350	0.6151
Injury, poisoning and procedural complications	0.5262	0.4947	0.5315	0.5943	0.5797
Task Average	0.5214	0.5073	0.5297	0.6071	0.6537

Elaboration of Model We elaborate the computing cost of Mo1eHD and compare it with SOTA neural networks. 1) Mo1eHD can leverage existing pre-trained **SMILES-PE** model on the general chemical dataset for pre-processing, i.e. such pre-trained model can be directly applied to any tasks without further pre-training effort. 2) For all the reported datasets, Mo1eHD is able to achieve the reported accuracy within 10 minutes using CPU only from the commodity desktop (AMD Ryzen™ 5 3600 3.6 GHz), note that this includes both training and inference for each dataset. 3) Mo1eHD also requires less space for model storage as for one binary classification task, model size of Mo1eHD is only around 80kB and during run-time, the memory footprint of Mo1eHD is also generally less than 10MB.

On the other hand, for GNN architectures as a comparison, extensive pre-training can be necessary, e.g., MolCLR requires around 5 days of pre-training using Nvidia® Quadro RTX™ 6000 as reported in the corresponding literature [37]. GNN models are also harder to implement considering the effort of establish multiple layers with considerable amount of nodes, especially the necessity of back-propagation during training with millions of parameters in total [23].

5.4 Limitations

The limitations of Mo1eHD come with the limitations of HDC. Compared with other machine learning algorithms such as neural networks, HDC is less application-agnostic thus the HDC operations are bind with physical meanings. Therefore, developing an HDC encoding scheme requires domain knowledge of the application, which could add more human effort. In addition, unlike DNNs having Tensorflow or Pytorch, currently there are no existing frameworks or libraries that can support the

development of HDC models. This calls for active follow-up research efforts from the machine learning and data science community.

6 Conclusion

In this paper, we propose and evaluate MoLeHD which leverages the novel brain-inspired hyperdimensional computing for molecule property prediction in drug discovery. MoLeHD projects SMILES strings of drug compound into hypervectors in the hyperdimensional space to extract features. The hypervectors are then used during training, retraining and inference of the HDC model to perform learning tasks. We evaluate MoLeHD on 30 classification tasks from 3 widely-used benchmark datasets and compare MoLeHD performance with 10 baseline machine learning algorithms including 6 SOTA neural network classifiers. Experimental results show that MoLeHD is able to outperform all the baseline models on average across the datasets consistently. In addition, MoLeHD also has other advantages such as less pre-processing efforts, smaller model size, faster run-time and stronger capability of generalization. This work marks the potential of using hyperdimensional computing as an alternative to the existing models in the drug discovery domain.

References

- [1] Roya Arian, Amirali Hariri, Alireza Mehridehnavi, Afshin Fassihi, and Fahimeh Ghasemi. Protein kinase inhibitors' classification using k-nearest neighbor algorithm. *Computational biology and chemistry*, 86:107269, 2020.
- [2] Elliot G Brown, Louise Wood, and Sue Wood. The medical dictionary for regulatory activities (meddra). *Drug safety*, 20(2):109–117, 1999.
- [3] Adrià Cereto-Massagué, María José Ojeda, Cristina Valls, Miquel Mulero, Santiago Garcia-Vallvé, and Gerard Pujadas. Molecular fingerprint similarity search in virtual screening. *Methods*, 71:58–63, 2015.
- [4] Andrew Dalke. Deepsmiles: An adaptation of smiles for use in. 2018.
- [5] Yin Fang, Haihong Yang, Xiang Zhuang, Xin Shao, Xiaohui Fan, and Huajun Chen. Knowledge-aware contrastive molecular graph learning. *arXiv preprint arXiv:2103.13047*, 2021.
- [6] Anna Gaulton, Louisa J Bellis, A Patricia Bento, Jon Chambers, Mark Davies, Anne Hersey, Yvonne Light, Shaun McGlinchey, David Michalovich, Bissan Al-Lazikani, et al. ChEMBL: a large-scale bioactivity database for drug discovery. *Nucleic acids research*, 40(D1):D1100–D1107, 2012.
- [7] Kaitlyn M Gayvert, Neel S Madhukar, and Olivier Elemento. A data-driven approach to predicting successes and failures of clinical trials. *Cell chemical biology*, 23(10):1294–1301, 2016.
- [8] Shion Honda, Shoi Shi, and Hiroki R Ueda. Smiles transformer: pre-trained molecular fingerprint for low data drug discovery. *arXiv preprint arXiv:1911.04738*, 2019.
- [9] Mohsen Imani, Samuel Bosch, Sohumi Datta, Sharadhi Ramakrishna, Sahand Salamat, Jan M Rabaey, and Tajana Rosing. Quanthd: A quantization framework for hyperdimensional computing. *IEEE Transactions on Computer-Aided Design of Integrated Circuits and Systems*, 39(10):2268–2278, 2019.
- [10] Mohsen Imani, Tarek Nassar, Abbas Rahimi, and Tajana Rosing. Hdna: Energy-efficient dna sequencing using hyperdimensional computing. In *2018 IEEE EMBS International Conference on Biomedical & Health Informatics (BHI)*, pages 271–274. IEEE, 2018.
- [11] Mohsen Imani, Abbas Rahimi, Deqian Kong, Tajana Rosing, and Jan M Rabaey. Exploring hyperdimensional associative memory. In *2017 IEEE International Symposium on High Performance Computer Architecture (HPCA)*, pages 445–456. IEEE, 2017.
- [12] PB Jayaraj, Mathias K Ajay, M Nufail, G Gopakumar, and UC Abdul Jaleel. Gpurfscreen: a gpu based virtual screening tool using random forest classifier. *Journal of cheminformatics*, 8(1):1–10, 2016.
- [13] Pentti Kanerva. Hyperdimensional computing: An introduction to computing in distributed representation with high-dimensional random vectors. *Cognitive computation*, 1(2):139–159, 2009.

- [14] Geethan Karunaratne, Manuel Le Gallo, Giovanni Cherubini, Luca Benini, Abbas Rahimi, and Abu Sebastian. In-memory hyperdimensional computing. *Nature Electronics*, 3(6):327–337, 2020.
- [15] Steven Kearnes, Kevin McCloskey, Marc Berndl, Vijay Pande, and Patrick Riley. Molecular graph convolutions: moving beyond fingerprints. *Journal of computer-aided molecular design*, 30(8):595–608, 2016.
- [16] Sunghwan Kim, Paul A Thiessen, Evan E Bolton, Jie Chen, Gang Fu, Asta Gindulyte, Lianyi Han, Jane He, Siqian He, Benjamin A Shoemaker, et al. Pubchem substance and compound databases. *Nucleic acids research*, 44(D1):D1202–D1213, 2016.
- [17] Denis Kleyko, Evgeny Osipov, Nikolaos Papakonstantinou, and Valeriy Vyatkin. Hyperdimensional computing in industrial systems: the use-case of distributed fault isolation in a power plant. *IEEE Access*, 6:30766–30777, 2018.
- [18] Michael Kuhn, Ivica Letunic, Lars Juhl Jensen, and Peer Bork. The sider database of drugs and side effects. *Nucleic acids research*, 44(D1):D1075–D1079, 2016.
- [19] Greg Landrum. Rdkit documentation. *Release*, 1(1-79):4, 2013.
- [20] Xinhao Li and Denis Fourches. Smiles pair encoding: A data-driven substructure tokenization algorithm for deep learning. 2020.
- [21] Chin Y Liew, Xiao H Ma, Xianghui Liu, and Chun W Yap. Svm model for virtual screening of lck inhibitors. *Journal of chemical information and modeling*, 49(4):877–885, 2009.
- [22] Xuan Lin, Zhe Quan, Zhi-Jie Wang, Huang Huang, and Xiangxiang Zeng. A novel molecular representation with bigru neural networks for learning atom. *Briefings in bioinformatics*, 21(6):2099–2111, 2020.
- [23] Hehuan Ma, Yatao Bian, Yu Rong, Wenbing Huang, Tingyang Xu, Weiyang Xie, Geyan Ye, and Junzhou Huang. Multi-view graph neural networks for molecular property prediction. *arXiv preprint arXiv:2005.13607*, 2020.
- [24] Ines Filipa Martins, Ana L Teixeira, Luis Pinheiro, and Andre O Falcao. A bayesian approach to in silico blood-brain barrier penetration modeling. *Journal of chemical information and modeling*, 52(6):1686–1697, 2012.
- [25] Andreas Mayr, Günter Klambauer, Thomas Unterthiner, Marvin Steijaert, Jörg K Wegner, Hugo Ceulemans, Djork-Arné Clevert, and Sepp Hochreiter. Large-scale comparison of machine learning methods for drug target prediction on chembl. *Chemical science*, 9(24):5441–5451, 2018.
- [26] Anton Mitrokhin, P Sutor, Cornelia Fermüller, and Yiannis Aloimonos. Learning sensorimotor control with neuromorphic sensors: Toward hyperdimensional active perception. *Science Robotics*, 4(30), 2019.
- [27] Justin Morris, Mohsen Imani, Samuel Bosch, Anthony Thomas, Helen Shu, and Tajana Rosing. Comphd: Efficient hyperdimensional computing using model compression. In *2019 IEEE/ACM International Symposium on Low Power Electronics and Design (ISLPED)*, pages 1–6. IEEE, 2019.
- [28] Gabriel A Pinheiro, Johnatan Mucelini, Marinalva D Soares, Ronaldo C Prati, Juarez LF Da Silva, and Marcos G Quiles. Machine learning prediction of nine molecular properties based on the smiles representation of the qm9 quantum-chemistry dataset. *The Journal of Physical Chemistry A*, 124(47):9854–9866, 2020.
- [29] Zhe Quan, Xuan Lin, Zhi-Jie Wang, Yan Liu, Fan Wang, and Kenli Li. A system for learning atoms based on long short-term memory recurrent neural networks. In *2018 IEEE International Conference on Bioinformatics and Biomedicine (BIBM)*, pages 728–733. IEEE, 2018.
- [30] Abbas Rahimi et al. Hyperdimensional biosignal processing: A case study for emg-based hand gesture recognition. In *ICRC*, 2016.
- [31] Abbas Rahimi, Pentti Kanerva, and Jan M Rabaey. A robust and energy-efficient classifier using brain-inspired hyperdimensional computing. In *Proceedings of the 2016 International Symposium on Low Power Electronics and Design*, pages 64–69, 2016.
- [32] Bharath Ramsundar, Peter Eastman, Patrick Walters, and Vijay Pande. *Deep learning for the life sciences: applying deep learning to genomics, microscopy, drug discovery, and more.* " O'Reilly Media, Inc.", 2019.

- [33] David Rogers and Mathew Hahn. Extended-connectivity fingerprints. *Journal of chemical information and modeling*, 50(5):742–754, 2010.
- [34] Sahand Salamat, Mohsen Imani, and Tajana Rosing. Accelerating hyperdimensional computing on fpgas by exploiting computational reuse. *IEEE Transactions on Computers*, 69(8):1159–1171, 2020.
- [35] Hongmao Sun. Pharmacophore-based virtual screening. *Current medicinal chemistry*, 15(10):1018–1024, 2008.
- [36] Kyle Swanson. *Message passing neural networks for molecular property prediction*. PhD thesis, Massachusetts Institute of Technology, 2019.
- [37] Yuyang Wang, Jianren Wang, Zhonglin Cao, and Amir Barati Farimani. Molclr: Molecular contrastive learning of representations via graph neural networks. *arXiv preprint arXiv:2102.10056*, 2021.
- [38] David Weininger. Smiles, a chemical language and information system. 1. introduction to methodology and encoding rules. *Journal of chemical information and computer sciences*, 28(1):31–36, 1988.
- [39] Tony F Wu et al. Brain-inspired computing exploiting carbon nanotube fets and resistive ram: Hyperdimensional computing case study. In *ISSCC*, 2018.
- [40] Zhenqin Wu, Bharath Ramsundar, Evan N Feinberg, Joseph Gomes, Caleb Geniesse, Aneesh S Pappu, Karl Leswing, and Vijay Pande. Moleculenet: a benchmark for molecular machine learning. *Chemical science*, 9(2):513–530, 2018.
- [41] Kevin Yang et al. *Are learned molecular representations ready for prime time?* PhD thesis, Massachusetts Institute of Technology, 2019.